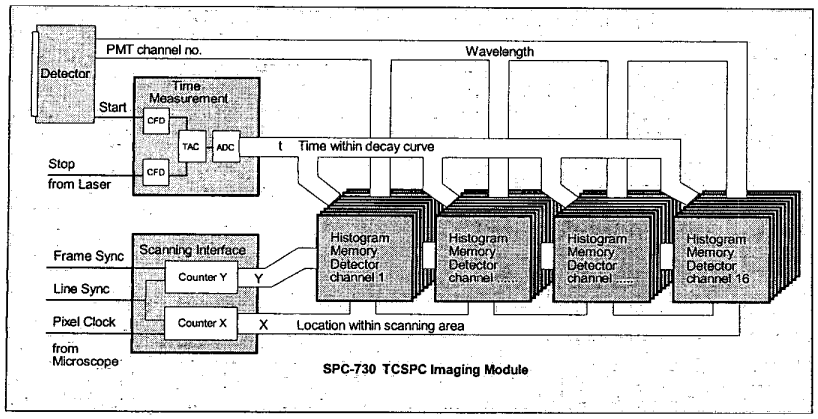

CWC5 Fig. 1. TCSPC Imaging.

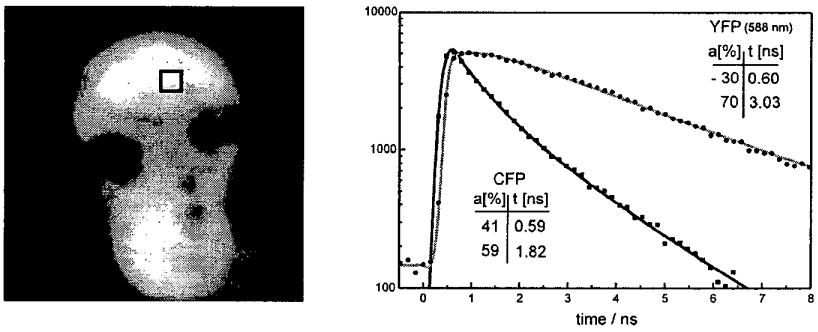

CWC5 Fig. 2. Intensity image of CFP and fluorescence decay curves of CFP and YFP in a selected region.

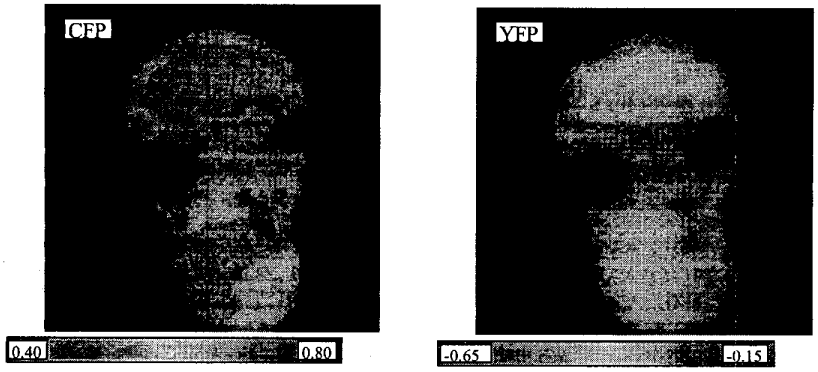

CWC5 Fig. 3. FRET images for CFP and YFP. Brightness = Intensity, Colour = Coefficient ratio for fast and slow decay component.

fixed link between the CFP and the YFP in the used cell the changes are relatively small.

FRET imaging by the coefficient ratio may be complicated by a possible short lifetime component of the CFP itself. However, data obtained by multicolour TCSPC imaging could help to tackle the general problem of the CFP lifetime in FRET systems.

3. Conclusions

A new TCSPC imaging technique in conjunction with a laser scanning microscope and a multi-channel PMT yields time- and wavelength resolved fluorescence images. Applied to FRET in living cells, the technique delivers the decay components of the donor and acceptor fluorescence in all pixels of the image. The data can be used to build up images showing the amount of FRET in the individual parts of the cell.

CWC6 **4:00 pm**

Nanometer X-ray Microscopy of Labeled Live Biological Organisms with a Nanosecond Laser-plasma Source

M.R. Al-Ani, J. Biggerstaff,# M. Trujillo, & M. Richardson, School of Optics & CREOL, University of Central Florida, Orlando, FL; #also of Dept Molecular & Microbiology, University of Central Florida, Orlando, Florida; Email: mrichard@mail.ucf.edu

One of the highest priorities of microbiology today is the need to visualize live microorganisms, such as single cells, bacteria, viruses, etc., with sufficient temporal and spatial resolution and specificity to understand their structural and functional dynamics. Protein-specific, fluorescence-labeling, or 'molecular-tagging' and laser-scanning confocal-optical-microscopy [LSCM] is currently used, but is limited in spatial resolution to ~200–300 nm.[1] X-ray microscopy [XRM] has achieved much higher spatial resolution[2], and x-ray labeling techniques have been used, with synchrotron sources[3]. However, these sources require exposure times of several seconds, and resort to rapid cryogenic freezing[4] of the specimen is needed for living organisms. Here we demonstrate, to our knowledge for the first time, the use of nanoparticle Au-labeling techniques in XRM using single, nanosecond, laser-plasma x-ray illumination of the specimen. In this case the specimen is in its natural state, and a high-resolution (~30 nm) x-ray radiograph is obtained in a time shorter than that required for any x-ray induced structural changes to the organism to be manifested on the image. Moreover we demonstrate, a technique in which *combined* labeled images of specific sites in the organism are obtained through both XRM and LSCM.

The sites of the organism to be imaged are identified by tagging them with particular antigens. In the two cases we have studied, melanoma tumor cells and human lymphocyte cells, mouse-α CD54 and CD3 antibodies respectively, were attached to antigens on the surface of the organism. To these antibodies were attached Oregon green dyed goat-α IgG antibodies, to provide a visible fluorescor for LSCM. Lastly, to these antibodies were then attached donkey-α goat antibodies seeded with 18 nm Au nanoparticles.

The laser-plasma XRM described here[5] utilizes plasma emission in the so-called 'water window' (2.3–4.5 nm) from an Yttrium target irradiated at 3×10^{12} W/cm^2 with 3J, 10 ns laser pulses from a Nd:glass laser.[6] The organisms, after sequential treatment by the three antibodies, are immersed in their natural fluid in a 10 μm-thick, vacuum-tight, specimen-cell having a 1 mm square, 100 nm thick SiN x-ray window, and, opposite it, a thin layer of PMMA photo-resist deposited on a Si substrate. The specimen cell is then exposed to one shot of the 100 μm diameter laser plasma x-ray source, and a transmission radiograph recorded on the photoresist. The high resolution image is thus recorded as a 1:1 registration of the line-of-sight absorptivity of the specimen. After development, the three-dimensional relief recorded on the photo-resist is analyzed with a high resolution atomic force microscope. Fig. 1 shows images of a melanoma tumor cell taken with both the XRM described above, and the LSCM. In Fig.1(a) is shown an x-ray

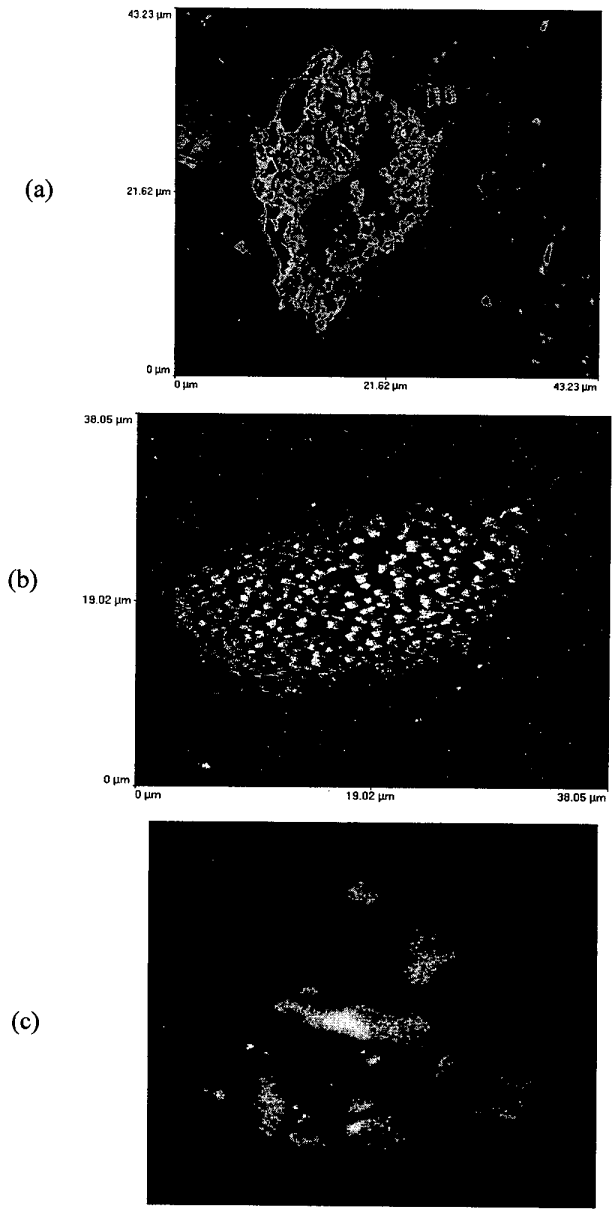

CWC6 Fig. 1. (a) X-ray microscope image of a melanoma cell without antibody tagging, (b) x-ray image of a similar cell with Au nano-particle antibody tagging (c) Confocal fluorescence microscope image of a similar melanoma cell.

image of the tumor cell without antibodies attached. Fig.1(b) shows a similar cell with the antibodies attached. The sites o local absorption by the 18 nm Au nanoparticles can clearly be seen. Fig. 1(c) show a comparable LSCM image of a similar cell. Although fluorescence from the visible molecular tags can clearly be seen, the resolution is limited. Similar images have been obtained with human lymphocyte cells.

We discuss the potential of this new form of high-resolution imaging, and describe measures made to quantify the structural effects identified by the nanoparticle x-ray tags.

References

1. J.B. Pawley, *Handbook of biological confocal microscopy,* 2nd ed., Plenum Press, NY. (1998).
2. G. Schneider & B. Neimann, "X-ray microscopy experiments with the X-ray microscope at the BESSY" in *X-ray Microscopy & Spectromicroscopy,* ed. J. Thieme, G. Schmahl, D. Randolph & E. Umbach, Publ. Springer Verlag, Berlin, p25, (1998).
3. H.N. Chapman, J.Fu, C. Jacbsen, and S. Williams, "Dark-Field X-ray Microscopy of Immunogold-labeled Cells," J. Microscopy Soc. Amer. 2, 23 (1996).
4. J. Maser, C. Jacobsen J. Kirz, et. al., "Development of a cryo scanning transmission x-ray microscope at NSLS" in *X-ray Microscopy & Spectromicroscopy,* ed. J. Thieme, G. Schmahl, D. Randolph & E. Umbach, Publ. Springer Verlag, Berlin, p 35, (1998).
5. M. Kado, M.C. Richardson, K. Gabel, D. Torres, J. Rajyaguru & M. Muszynski, "Ultra-structural imaging and molecular modeling of live bacteria using soft x-ray contact microscopy with nanoseconds laser plasma radiation", *Proc. SPIE,* 2523, 194, (1995).
6. V.P. Yanovsky, M.C. Richardson & E.J. Miesak, "Compact Single Frequency High Power Nd:Glass Laser", *IEEE J Quant. Electron.* 30, 884, (1994).

CWD 2:30 pm–4:15 pm
Room: 102

Optical Amplifiers

Peter Zory, Univ. of Florida, USA, Presider

CWD1 2:30 pm

High Average-power, Low-jitter, 10-GHz Semiconductor Modelocked Laser System

A. Braun, M. Kwakernaak, and J.H. Abeles, Sarnoff Corporation, 201 Washington Road, Princeton, NJ 08901, Email: abraun@sarnoff.com

C. DePriest, T. Yilmaz, and P. Delfyett, Jr., CREOL, University of Central Florida, 4000 Central Florida Blvd., Orlando, FL 32816

Introduction

To date, there has been a large body of work describing the generation of ultrashort and high power pulses from semiconductor gain elements.[1–4] Recently, however, there has been a growing interest in the development of ultra-low-jitter optical pulse sources for use in analog-to-digital conversion of wide-band RF signals, enabling sampling resolution greater than that obtained in high-speed electronic comparators.[5–9] Specifically, 10-Gbps pulse trains with 10-fs of timing jitter could provide for 12-bit A/D conversion of 5-GHz signals. Providing a compact source of low-jitter pulses, modelocked semiconductor lasers may provide the needed sampling pulses for such an application.[10,11] Implementation of these ultra-stable lasers in an optical A/D system requires that attention be paid not only to sampling aperture and stability, but to the optical power as well. In fact, the energy needed in each sampling pulse must be large enough such that the shot-noise generated upon detection is less than the least significant bit of the A/D converter. This requirement sets a lower limit on the needed pulse energy, and depending on the linearity of the modulation scheme, can be prohibitive.[12] Utilizing a linearized modulation scheme such as phase-encoded optical sampling,[12] 10-Gsps pulse trains with energies of 10 pJ/pulse can achieve a 10-bit sampling accuracy when the depth of modulation approaches 15%.

Experiment

The development of an all semiconductor-based 10-GHz repetition rate, 100-mW average power, sub 60-fs jitter pulse train is shown. All devices described are ridge-guided single mode waveguides. Modelocked pulses at 1.55 µm were generated from a harmonically modelocked external cavity with fundamental frequency of 1-GHz. A low-capacitance, two-section curved waveguide gain element (Figure 1) was utilized to actively modelock the cavity at 10-GHz by driving the